

Analysis of complex parametric vibrations of plates and shells using Bubnov-Galerkin approach

J. Awrejcewicz, A. V. Krysko

Summary The Bubnov-Galerkin method is applied to reduce partial differential equations governing the dynamics of flexible plates and shells to a discrete system with finite degrees of freedom. Chaotic behaviour of systems with various degrees of freedom is analysed. It is shown that the attractor dimension of a system has no relationship with the attractor dimension of any of its subsystems.

Keywords Shell, Bubnov-Galerkin method, Runge-Kutta method, Poincaré section, Lyapunov exponent, Chaotic vibration

1

Multibody dynamical systems

Chaotic vibrations exhibited by lumped systems with many degrees of freedom (DOF) are rarely investigated. Recently, however remarkable progress has been observed: hydrodynamic processes governed by ordinary differential equations (ODE) have been investigated within this field in [1–3]; finite-dimensional models of Ginzburg-Landau equations discretized with respect to spatial coordinates, multidimensional models of radiophysical systems governing the dynamics of coupled oscillators and generators as well as chains of oscillators and generators have been analysed in [4] and [5–7]. Most of the cited works addressed the problem of modeling a continuous system by a lumped (discrete) system governed by ODEs.

There is a wide gap however between finite- and infinite-dimensional models exhibiting chaotic dynamics: it begins at one and a half DOF and ends with systems governed by partial differential equations (PDE), e.g. of the Navier-Stokes type. In the DOF interval $[1.5; +\infty]$, of various systems, our attention is focused on structures governed by the von Kármán equation, which also belongs to the class of equations with these properties. This equation plays an important role in both mathematics and mechanics, [8–12].

In order to follow qualitative behaviour of various PDEs governing dynamics of continuous systems, a concept of phase space is used and infinite-dimensional systems are replaced by finite-dimensional ones governed by ODEs, [12–14].

However, two important questions appear which require clarification in order to address properly the stated problem.

First, infinite-dimensional systems of equations are truncated in the procedure, i. e. finite-dimensional systems are considered. It is arbitrarily assumed that an increase of the number of equations leads (beginning from a certain value) to stabilization of the system properties, and,

Received 22 October 2002; accepted for publication 9 July 2003

J. Awrejcewicz (✉)
Department of Automatics and Biomechanics,
Technical University of Lodz,
1/15 Stefanowskiego St., 90–924 Lodz, Poland
e-mail: awrejcew@ck-sg.p.lodz.pl

A. V. Krysko
Department of Mathematics,
Saratov State University, B. Sadovaja 96^A, f. 77
410054 Saratov, Russia
e-mail: tak@san.ru

This work has been partially supported by Department of Mathematics of the Central European University in Budapest.

hence, a further increase of the number of equations does not introduce anything new from both qualitative and quantitative points of view. This approach is motivated by the occurrence of finite-dimensional attractors exhibited by the original system. However, even if the attractors' dimension is bounded, it seems that more important influences on the results may have a way of carrying out the discussed truncation procedure. It is observed, that in the case of improper choice of a basis used for projection into the space of ODEs the obtained truncated system may have qualitatively different attractors in comparison to the attractors exhibited by the initial system.

This behaviour has been already observed in the analysis of two-dimensional equations governing the heat transfer of fluids. The Lorenz system, yielded by such truncation, exhibits chaotic dynamics. However, an increase of the modes number yields at first more intensive chaotic behaviour; further increase of the number of modes practically dampens the chaotic orbits. For a sufficiently high number of modes, the chaos disappears.

It has been shown in Ref. [1] that for a large Prandtl number δ in the analysed Boussinesque convection there are critical values of the Rayleigh number R_a , which are related to the occurrence of single and bi-modal vibrations. A further increase of R_a forces the system to return to a single-frequency periodic convection.

These examples yield an important observation: in order to have reliable and qualitatively similar results for both the original and the truncated systems, a rather high number of modes is required while applying the Bubnov-Galerkin approach. Recall that usually dynamic behaviour is simple when it is a stable one-frequency process. How many ODEs are needed, however, for a proper qualitative description of continuous systems with irregular dynamics?

The second important step in the approximation of a continuous system by a discretized one concerns the structure of the analysed system. The situation depends radically on whether or not the initial system is composed of interacting subsystems.

Note that the two illustrated purely theoretical events are rarely met in real situations. Consider a set of systems with independent dynamics, occupying uncoupled spaces A_1, A_2, \dots, A_N by the physical space. The frequency spectrum of the whole system consists of subsystems spectra. One may expect that an introduction of small couplings between subsystems also yields slight changes of the frequency spectrum, [15]. However, beginning from a certain coupling magnitude, the synchronization may occur between various parts of the coupled systems. The described synchronization during interactions of the subsystems with chaotic dynamics is observed either in a chain of autogenerators or oscillators, [16, 17].

It means that a dimension of an attractor of a whole system consisting of the set of subsystems may be reduced to an attractor dimension of one of the subsystems. However, when a synchronization of subsystems does not appear, the system's attractor dimension is equal to the sum of attractors dimensions of subsystems. Furthermore, if it is impossible to extract the subsystems, the mutual independence of any two subsystems may be estimated by a self-correlation function characterizing the dynamics of those two subsystems.

The discussed problem plays an essential role in the reconstruction of both the phase portraits of the system and its dimension. Usually, one-dimensional realization of a certain characteristic is applied and measured in a localized part of the phase space. The result obtained during analysis of such realizations yields the whole system dynamics, assuming that there is a space coherence or subsystems synchronization.

This approach is easily applicable e.g. to experimental investigations of the Belousov-Zhabotinsky reaction, [18]. However, in many hydrodynamical systems like the Couette flow, the experimentally recovered phase portraits and computation of a dimension with the lack of the data describing full space flow coherence hold only for dynamics of the local objects.

Since an attractor dimension in spatially distributed unsynchronized systems may increase unbounded, a fundamental question appears: how large may be the maximal attractors' dimension in unidirectionally coupled infinite-dimensional systems with fully synchronized dynamics, and in continuous systems with space coherence of dynamical regimes?

In this work, the complex dynamics of a continuous system is investigated using the example of a longitudinally harmonically excited rectangular plate.

In computations of non-linear dynamics of real shells, one has to address the key problem of the theory of continuous systems, i.e. the modeling of an investigated structure. The choice of an idealized lumped physical model is expected to sufficiently represent the properties of the original system, while remaining relatively simple in mathematical relations.

Recall that a shell (or any other structure) is characterized by an infinite spectrum of eigenfrequencies. Therefore, one could artificially construct an infinite series of lumped

(discrete) vibrating systems with one DOF. Where each single-DOF system would have the eigenfrequencies taken from the infinite spectrum of shell eigenfrequencies. Limiting the considerations to a finite number of such simple oscillators (for example, $M_x \times M_y$), which defines the DOF of the approximated system, the problem could be reduced to the analysis of $M_x \times M_y$ coupled nonlinear second-order ODEs. It is clear that an increase of the number $M_x \times M_y$, i.e. the number of the independent coordinates, would increase the quality of the approximation.

Nowadays, various approximative methods are applied to construct lumped systems. In this work, we use the Bubnov-Galerkin method, which has been successfully applied to different types of differential equations. In Ref. [16], a review of the Bubnov-Galerkin method (BGM) is given including a discussion of its convergence for various classes of differential equations. In Refs. [19, 20], the rate of convergence of the BGM for hyperbolic equations and for the coupled system of equations governing thermoelastic problems is also addressed.

2 Problem formulation and the Bubnov-Galerkin method

A shallow isotropic shell creating a closed three-dimensional space in R^3 is considered, Fig. 1. A rectangular coordinate system is attached to the shell. In the shell body, the mean surface $z = 0$ is introduced, and the direction of the axes Ox and Oy are associated with the main shell curvatures. In the given coordinate system, the shell is represented by the space $\Omega = \{(x, y, z) / (x, y) \in [0, 1] \times [0, 1], -h \leq z \leq h\}$, where the domain $[0, 1] \times [0, 1]$ represents the rectangular mean surface.

The equations governing dynamics of a rectangular shell, including both transversal and longitudinal harmonic excitations, have the following form, [16]:

$$\frac{\partial^2 w}{\partial t^2} + \varepsilon \frac{\partial w}{\partial t} + \frac{1}{12(1-\nu^2)} \left[\frac{1}{\lambda^2} \frac{\partial^4 w}{\partial x^4} + \lambda^2 \frac{\partial^4 w}{\partial y^4} + 2 \frac{\partial^4 w}{\partial x^2 \partial y^2} \right] + \left[P_x \frac{\partial^2 w}{\partial x^2} + P_y \frac{\partial^2 w}{\partial y^2} \right] - L(w, F) - \nabla_k^2 F + k_x P_x + k_y P_y - q = 0, \quad (1)$$

$$\frac{1}{\lambda^2} \frac{\partial^4 F}{\partial x^4} + \lambda^2 \frac{\partial^4 F}{\partial y^4} + 2 \frac{\partial^4 F}{\partial x^2 \partial y^2} + \nabla_k^2 w + \frac{1}{2} L(w, w) = 0, \quad (2)$$

where

$$\nabla_k^2 = k_x \frac{\partial^2}{\partial x^2} + k_y \frac{\partial^2}{\partial y^2},$$

$$L(w, w) = 2 \left[\frac{\partial^2 w}{\partial x^2} \frac{\partial^2 w}{\partial y^2} - \left(\frac{\partial^2 w}{\partial x \partial y} \right)^2 \right], \quad (3)$$

$$L(w, F) = \frac{\partial^2 w}{\partial x^2} \frac{\partial^2 F}{\partial y^2} + \frac{\partial^2 w}{\partial y^2} \frac{\partial^2 F}{\partial x^2} - 2 \frac{\partial^2 w}{\partial x \partial y} \frac{\partial^2 F}{\partial x \partial y}.$$

The system of equations (1) and (2) is already in the nondimensional form, whereas the relations between dimensional and nondimensional parameters read

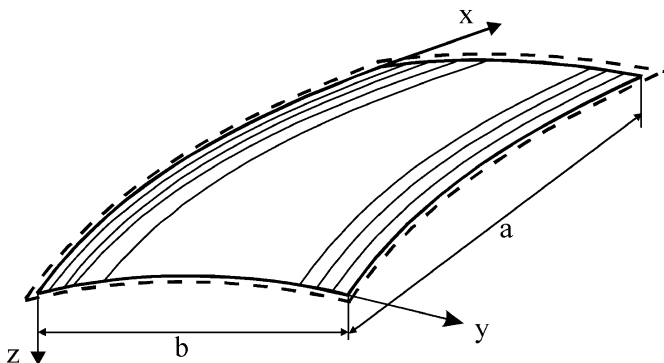


Fig. 1. The analysed shell

$$\begin{aligned}
w &= 2h\bar{w}, \quad x = a\bar{x}, \quad y = b\bar{y}, \quad \lambda = \frac{a}{b}, \quad F = E(2h)^3\bar{F}, \\
k_x &= \frac{2h}{a^2}\bar{k}_x, \quad k_y = \frac{2h}{b^2}\bar{k}_y, \quad q = \frac{E(2h)^4}{a^2b^2}\bar{q}, \\
t &= \frac{ab}{2h}\sqrt{\frac{\rho}{E}}\bar{t}, \quad \varepsilon = \frac{2h}{ab}\sqrt{\frac{E}{\rho}}\bar{\varepsilon}, \quad P_x = \frac{E(2h)^3}{b^2}\bar{P}_x, \quad P_y = \frac{E(2h)^3}{a^2}\bar{P}_y.
\end{aligned} \tag{4}$$

In the above, w and F denote the deflection and the stress functions, respectively; $2h$ is the shell thickness; a, b are the shell dimensions; $k_x = R_x^{-1}$, $k_y = R_y^{-1}$ denote the shell curvatures along x and y , respectively; ρ is the shell mass density; E denotes Young modulus; ν is Poisson's coefficient of the isotropic material; P_x, P_y are the longitudinal loads along x, y axes, respectively; q is the transversal distributed load.

Note that quantities with bars in (4) are nondimensional (bars are omitted in equations (1)–(3)).

Let us denote the left-hand sides of Eqs. (1) and (2) by Φ_1 and Φ_2 , respectively. Hence, the equations have the form

$$\begin{aligned}
\Phi_1 \left(\frac{\partial^2 w}{\partial^2 x}, \frac{\partial^2 F}{\partial^2 x}, k_x, k_y, P_x, P_y, q, t, \dots \right) &= 0, \\
\Phi_2 \left(\frac{\partial^2 w}{\partial^2 x}, \frac{\partial^4 F}{\partial^4 x}, k_x, k_y, \dots \right) &= 0.
\end{aligned} \tag{5}$$

In addition, the corresponding boundary conditions should be attached. Since the exact solution of the formulated boundary value problem is not known, the BGM method with higher approximations is applied. We assume the following form of the unknown functions

$$\begin{aligned}
w &= \sum_{ij} A_{ij}(t)\varphi_{ij}(x, y), \\
F &= \sum_{ij} B_{ij}(t)\psi_{ij}(x, y), \\
i &= 1, 2, \dots, M_x; \quad j = 1, 2, \dots, M_y.
\end{aligned} \tag{6}$$

Applying the BGM procedure to Eqs. (5), one obtains

$$\begin{aligned}
\int_0^1 \int_0^1 \phi_1 \varphi_{vz}(x, y) dx dy &= 0, \\
\int_0^1 \int_0^1 \phi_2 \psi_{vz}(x, y) dx dy &= 0, \\
v &= 1, 2, \dots, M_x; \quad z = 1, 2, \dots, M_y,
\end{aligned} \tag{7}$$

or, taking into account (6), we get

$$\begin{aligned}
\sum_{vz} \left[\sum_{ij} \left(\frac{d^2 A_{ij}}{dt^2} + \varepsilon \frac{dA_{ij}}{dt} - q + k_x P_x + k_y P_y \right) I_{3,vzij} + \sum_{ij} A_{ij} I_{1,vzij} \right. \\
\left. - \sum_{ij} B_{ij} I_{2,vzij} + \sum_{ij} A_{ij} I_{5,vzij} - \sum_{ij} A_{ij} \sum_{kl} B_{kl} I_{4,vzijkl} \right] = 0,
\end{aligned} \tag{8}$$

$$\begin{aligned}
\sum_{vz} \left[\sum_{ij} A_{ij} I_{7,vzij} + \sum_{ij} B_{ij} I_{8,vzij} + \sum_{ij} A_{ij} \sum_{kl} A_{kl} I_{6,vzijkl} \right] = 0, \\
v, i, k = 1, 2, \dots, M_x; \quad z, j, l = 1, 2, \dots, M_y
\end{aligned} \tag{9}$$

The integrals of the BGM procedure are:

$$I_{1,vzij} = \int_0^1 \int_0^1 \frac{1}{12(1-v^2)} \left[\frac{1}{\lambda^2} \frac{\partial^4 \varphi_{ij}}{\partial x^4} + \lambda^2 \frac{\partial^4 \varphi_{ij}}{\partial y^4} + 2 \frac{\partial^4 \varphi_{ij}}{\partial x^2 \partial y^2} \right] \varphi_{vz} \, dx \, dy \, , \quad (10)$$

$$I_{2,vzij} = \int_0^1 \int_0^1 \left[k_y \frac{\partial^2 \psi_{ij}}{\partial x^2} + k_x \frac{\partial^2 \psi_{ij}}{\partial y^2} \right] \varphi_{vz} \, dx \, dy \, , \quad (11)$$

$$I_{3,vzij} = \int_0^1 \int_0^1 \varphi_{vz} \, dx \, dy \, , \quad (12)$$

$$I_{4,vzijkl} = \int_0^1 \int_0^1 \left[\frac{\partial^2 \varphi_{ij}}{\partial x^2} \frac{\partial^2 \psi_{kl}}{\partial y^2} + \frac{\partial^2 \varphi_{ij}}{\partial y^2} \frac{\partial^2 \psi_{kl}}{\partial x^2} - 2 \frac{\partial^2 \varphi_{ij}}{\partial x \partial y} \frac{\partial^2 \psi_{kl}}{\partial x \partial y} \right] \varphi_{vz} \, dx \, dy \, , \quad (13)$$

$$I_{5,vzij} = \int_0^1 \int_0^1 \left[\frac{\partial^2 \varphi_{ij}}{\partial x^2} P_x + \frac{\partial^2 \varphi_{ij}}{\partial y^2} P_y \right] \varphi_{vz} \, dx \, dy \, , \quad (14)$$

$$I_{6,vzijkl} = \int_0^1 \int_0^1 \left[\frac{\partial^2 \varphi_{ij}}{\partial x^2} \frac{\partial^2 \varphi_{kl}}{\partial y^2} - \frac{\partial^2 \varphi_{ij}}{\partial x \partial y} \frac{\partial^2 \varphi_{kl}}{\partial x \partial y} \right] \psi_{vz} \, dx \, dy \, , \quad (15)$$

$$I_{7,vzij} = \int_0^1 \int_0^1 \left[k_y \frac{\partial^2 \varphi_{ij}}{\partial x^2} + k_x \frac{\partial^2 \varphi_{ij}}{\partial y^2} \right] \psi_{vz} \, dx \, dy \, , \quad (16)$$

$$I_{8,vzij} = \int_0^1 \int_0^1 \left[\frac{1}{\lambda^2} \frac{\partial^4 \psi_{ij}}{\partial x^4} + \lambda^2 \frac{\partial^4 \psi_{ij}}{\partial y^4} + 2 \frac{\partial^4 \psi_{ij}}{\partial x^2 \partial y^2} \right] \psi_{vz} \, dx \, dy \, . \quad (17)$$

The integrals (10)–(17), except for possibly $I_{3,vzij}$ (if the transversal load q is applied not to the whole shell surface), are computed for the entire middle surface.

To conclude, the derived system consists of $M_x \times M_y$ second-order ODEs (8) with respect to the time-dependent function A_{ij} and of linear algebraic equations (9) with respect to B_{ij} for each time instance.

The initial conditions have the following form

$$w \Big|_{t=0} = w_0, \quad \frac{dw}{dt} \Big|_{t=0} = 0 \, , \quad (18)$$

where w_0 is either taken from the corresponding static problem or is otherwise defined.

Assuming the loading terms, the system of equations (8) and (9) is solved numerically, to obtain A_{ij} and B_{ij} . Next, the found values of A_{ij} and B_{ij} are substituted into (6), and the sought functions w, F can be finally recovered.

3

Numerical experiment

First, we present the numerical algorithm. Both functions φ_{ij} and ψ_{ij} from (6) are represented in the multiplicative forms of a product of two functions depending only on one argument. They may be given in the form

$$\begin{aligned} \varphi_{ij}(x, y) &= \varphi_{1i}(x) \varphi_{2j}(y), \\ \psi_{ij}(x, y) &= \psi_{1i}(x) \psi_{2j}(y) \, , \end{aligned} \quad (19)$$

to satisfy the following two types of boundary conditions:

$$\begin{aligned} w = 0, \quad \frac{\partial^2 w}{\partial x^2} = 0, \quad F = 0, \quad \frac{\partial^2 F}{\partial x^2} = 0 \quad \text{for } x = 0; 1, \\ w = 0, \quad \frac{\partial^2 w}{\partial y^2} = 0, \quad F = 0, \quad \frac{\partial^2 F}{\partial y^2} = 0 \quad \text{for } y = 0; 1 . \end{aligned} \quad (20)$$

Substituting (20) into (19) we obtain

$$\begin{aligned} \varphi_{1i}(x) = \psi_{1i}(x) = \sin(i\pi x), \quad i = 1, 2, \dots, M_x, \\ \varphi_{2j}(y) = \psi_{2j}(y) = \sin(j\pi y), \quad i = 1, 2, \dots, M_y , \end{aligned} \quad (21)$$

whereas, substituting (21) into (6), we get

$$\begin{aligned} w = \sum_{ij} A_{ij}(t) \sin(i\pi x) \sin(j\pi y), \\ F = \sum_{ij} B_{ij}(t) \sin(i\pi x) \sin(j\pi y) . \end{aligned} \quad (22)$$

In the above, the indices i, j take all admissible values.

Substituting (22) into (7) and (8) and taking into account the BGM with higher approximations we obtain a system of second-order ODEs (next reduced to a normal form) and, system of linear algebraic equations with respect to $B_{ij}(t)$, .

The system of ODEs is solved using the fourth-order Runge-Kutta procedures with a constant time-step, which is defined using the Runge's rule. At each of the integration steps, the following algebraic system of equations:

$$\int_0^1 \int_0^1 \phi_1 \sin(v\pi x) \sin(z\pi y) dx dy = 0 , \quad (23)$$

$$\int_0^1 \int_0^1 \phi_2 \sin(v\pi x) \sin(z\pi y) dx dy = 0, \quad v = 1, 2, \dots, M_x; \quad z = 1, 2, \dots, M_y , \quad (24)$$

is solved using the Gauss method. Integrals of the BGM are expressed by the formulas

$$I_{1,v} = -\frac{1}{v\pi} [\cos(v\pi x_2) - \cos(v\pi x_1)] , \quad (25)$$

$$I_{2,z} = -\frac{1}{z\pi} [\cos(z\pi y_2) - \cos(z\pi y_1)] , \quad (26)$$

$$I_{3,vi} = \begin{cases} \frac{1}{2}, & i = v, \\ 0, & i \neq v , \end{cases} \quad (27)$$

$$I_{4,zj} = \begin{cases} \frac{1}{2}, & j = z, \\ 0, & j \neq z , \end{cases} \quad (28)$$

$$I_{5,vik} = \begin{cases} \frac{1}{4\pi} \left[-\frac{\cos(\alpha_1\pi)}{\alpha_1} - \frac{\cos(\alpha_2\pi)}{\alpha_2} - \frac{\cos(\alpha_3\pi)}{\alpha_3} + \frac{\cos(\alpha_4\pi)}{\alpha_4} + \frac{1}{\alpha_1} + \frac{1}{\alpha_2} + \frac{1}{\alpha_3} - \frac{1}{\alpha_4} \right], & \alpha_l \neq 0; \\ \left[\frac{\cos \alpha_l \pi}{\alpha_l} = 0, \frac{1}{\alpha_l} = 0 \right], & l = 1, 2, 3; \alpha_l = 0 ; \end{cases} \quad (29)$$

where

$$\begin{aligned} \alpha_1 = i + k - v, \quad \alpha_2 = k + v - i, \\ \alpha_3 = v + i - k, \quad \alpha_4 = i + k + v, \end{aligned}$$

$$I_{6,zjl} = \begin{cases} \frac{1}{4\pi} \left[-\frac{\cos(\beta_1\pi)}{\beta_1} - \frac{\cos(\beta_2\pi)}{\beta_2} - \frac{\cos(\beta_3\pi)}{\beta_3} + \frac{\cos(\beta_4\pi)}{\beta_4} + \frac{1}{\beta_1} + \frac{1}{\beta_2} + \frac{1}{\beta_3} - \frac{1}{\beta_4} \right], & \beta_l \neq 0; \\ \left[\frac{\cos\beta_l\pi}{\beta_l} = 0, \frac{1}{\beta_l} = 0 \right], & l = 1, 2, 3; \beta_l = 0; \end{cases} \quad (30)$$

where

$$\begin{aligned} \beta_1 &= j + l - z, & \beta_2 &= l + z - j, \\ \beta_3 &= z + j - l, & \beta_4 &= j + l + z, \end{aligned}$$

$$I_{7,vik} = \begin{cases} \frac{1}{4\pi} \left[-\frac{\cos(\alpha_1\pi)}{\alpha_1} - \frac{\cos(\alpha_2\pi)}{\alpha_2} - \frac{\cos(\alpha_3\pi)}{\alpha_3} - \frac{\cos(\alpha_4\pi)}{\alpha_4} - \frac{1}{\alpha_1} + \frac{1}{\alpha_2} + \frac{1}{\alpha_3} - \frac{1}{\alpha_4} \right], & \alpha_l \neq 0; \\ \left[\frac{\cos\alpha_l\pi}{\alpha_l} = 0, \frac{1}{\alpha_l} = 0 \right], & l = 1, 2, 3; \alpha_l = 0; \end{cases} \quad (31)$$

$$I_{8,zjl} = \begin{cases} \frac{1}{4\pi} \left[\frac{\cos(\beta_1\pi)}{\beta_1} - \frac{\cos(\beta_2\pi)}{\beta_2} - \frac{\cos(\beta_3\pi)}{\beta_3} - \frac{\cos(\beta_4\pi)}{\beta_4} - \frac{1}{\beta_1} + \frac{1}{\beta_2} + \frac{1}{\beta_3} + \frac{1}{\beta_4} \right], & \beta_l \neq 0; \\ \left[\frac{\cos\beta_l\pi}{\beta_l} = 0, \frac{1}{\beta_l} = 0 \right], & l = 1, 2, 3; \beta_l = 0, \end{cases} \quad (32)$$

where x_1, x_2, y_1, y_2 are coordinates of the rectangular area of the normal load input q .

The following notation is introduced:

$$I_{Q,vz} = I_{1,v}I_{2,z}, \quad I_{AB,vz} = (z^2k_x + v^2k_y)\pi^2I_{3,vi}I_{4,zj}, \quad (33)$$

$$I_{vzijkl} = \pi^4[(i^2l^2 + j^2k^2)I_{5,vik}I_{6,zjl} - 2ijklI_{7,vik}I_{8,zjl}], \quad (34)$$

$$J_{1,vzij} = \frac{\pi^4}{12(1-\mu^2)} \left[\frac{v^4}{\lambda^2} + 2v^2z^2 + \lambda^2z^4 \right] I_{3,vi}I_{4,zj}, \quad (35)$$

$$J_{2,vzij} = [v^2P_x + z^2P_y]\pi^2I_{3,vi}I_{4,zj},$$

$$J_{3,vzij} = \left[\frac{v^4}{\lambda^2} + 2v^2z^2 + \lambda^2z^4 \right] \pi^4I_{3,vi}I_{4,zj}. \quad (36)$$

Taking into account the given integrals, the system (8) and (9) takes the form

$$\begin{aligned} \sum_{ij} \left[\frac{d^2A_{vz}}{dt^2} I_{3,vi}I_{4,zj} - \varepsilon \frac{dA_{vz}}{dt} I_{3,vi}I_{4,zj} - A_{vz}(J_{1,vzij} - J_{2,vzij}) - B_{vz}I_{AB,vz} \right. \\ \left. + qI_{Q,vz} - (k_xP_x + k_yP_y)I_{3,vi}I_{4,zj} + A_{ij} \sum_{kl} B_{kl}I_{vzijkl} \right], \end{aligned} \quad (37)$$

$$\sum_{ij} [B_{vz}J_{3,vzij} - A_{vz}I_{AB} + \frac{1}{2}A_{ij} \sum_{kl} A_{kl}I_{vzijkl}] = 0. \quad (38)$$

Runge's note is applied to secure a proper choice of the time-step of computations using the Runge-Kutta method. Namely, we compare the results obtained for time steps Δt and $2\Delta t$. If they overlap, then the computational step Δt is applied. Runge's rule is also applied while representing a solution by series (21) and (22), i.e. computational results are compared for different M_x, M_y and $M_x - 1, M_y - 1$.

When only a longitudinal load is applied, the initial form of the deflection surface is given via the initial condition of the initial problem (18), i. e. we take $A_{11} = 0.0001$.

Results and discussions

As an example, a square plate ($\lambda = 1, \varepsilon = 1$), supported by balls on its contour on flexible nonstretched (noncompressed) ribs (20) and excited longitudinally by $P_x = P_{x_0}(1 - \sin \omega_2 t)$ is investigated. The computations are carried out for fixed ω_2 with variations of the control parameter $P_{x_0} = 1 \pm 18$. The numerical results are used to construct the dependencies $w_{\max}(P_{x_0}), w_{ij}(\dot{w}_{ij})$, the power spectrum, the Poincaré sections and the Lyapunov exponents.

Some of these characteristics are shown in Fig. 2 and Table 1. In Fig. 2, the dependence of maximal deflection in the center of the square plate, versus the longitudinal load P_{x_0} , is reported. Curve 1 is obtained using a first-order approximation (i. e. $i = j = 1$ in relation (22)); curve 2 is obtained using the 9th-order approximation ($i = j = 3$); curve 3 is obtained using the 25th-order approximation ($i = j = 5$); and finally, curve 4 is obtained using 49th-order approximation ($i = j = 7$). The derived results are divided into four intervals:

$I - 1 \leq P_{x_0} \leq 4.5$, $II - 4.5 \leq P_{x_0} \leq 5.5$, $III - 5.5 \leq P_{x_0} \leq 7.5$, $IV - 7.5 \leq P_{x_0} \leq 18.5$.

The intervals $0 \leq P_{x_0} \leq 1$ and II correspond to intervals of stable equilibrium. In the interval $I-II$, for all approximations, the same results are obtained (practically) for all earlier mentioned characteristics: the dependencies $(w_{ij}(t)), (\dot{w}_{ij}(t))$, the power spectra, Poincaré sections and Lyapunov exponents. In the interval III , practically acceptable results are achieved when forty nine series terms are used.

In Table 1, a convergence of the Bubnov-Galerkin method with respect to deflection function depending on the terms number in series (21) and (22) for $P_{x_0} = 5.65$ and $P_{x_0} = 18$ is discussed. It is worth noticing that for $P_{x_0} = 5.65$, the first approximation, i.e. one-mode solution, essentially differs from that of $M_x = M_y = 3$ (nine modes), $M_x = M_y = 5$ (twenty five modes), and $M_x = M_y = 7$ (forty nine modes). However, already for $M_x = M_y = 3, 5, 7$, the results overlap in full with respect to all applied analysis tools (phase portraits, signals, power spectra and Lyapunov exponents), i.e. in practice an exact solution is obtained. Observe that for a given value $P_{x_0} = 5.65$, one may get practically an exact solution applying nine modes ($M_x = M_y = 3$). Owing to the analysis of fundamental results for $P_{x_0} = 18$ given in Table 1, one may conclude that the first approximation (one-mode solution) yields take results (harmonic solution) when increasing number of series (21), (22) terms and beginning from $M_x = M_y = 3, 5, 7$ a chaotic vibration regime is exhibited, which is indicated by the used numerical characteristics (phase portraits, power spectra, Poincaré sections and Lyapunov exponents). It should be emphasized that the signal associated with the use of $M_x = M_y = 3, 5, 7$ is strictly chaotic.

In the next step, a contribution of each mode to the vibrational regime has been also analysed. In this case, the first mode computations coincide beginning from $M_x = M_y = 3$.

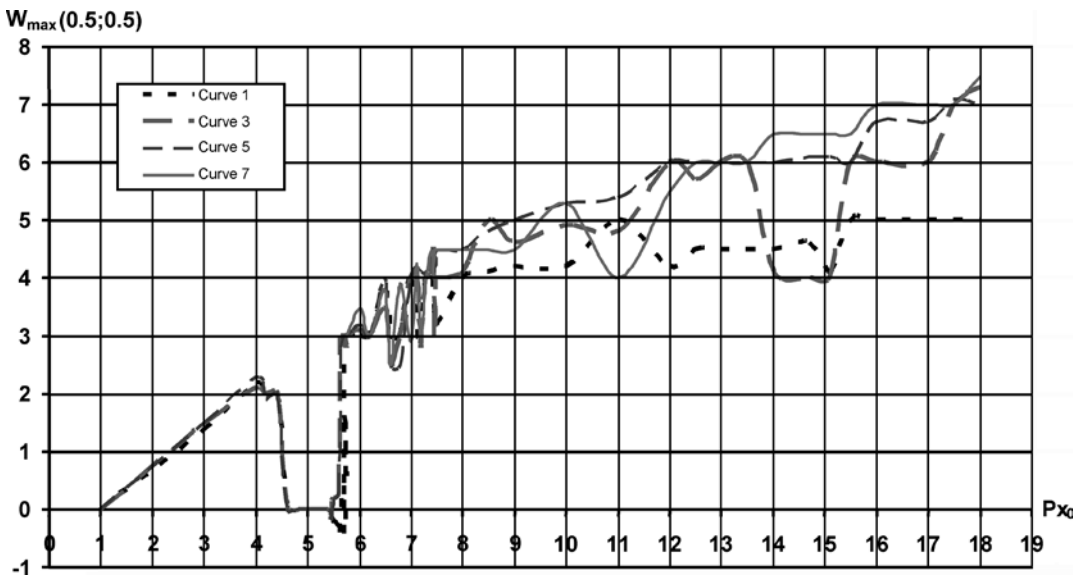
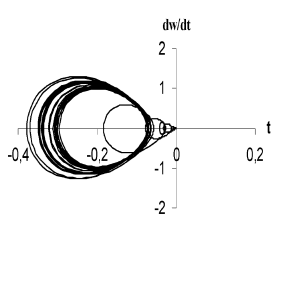
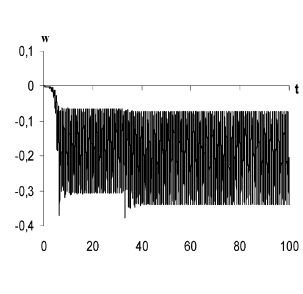
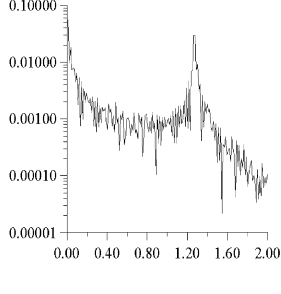
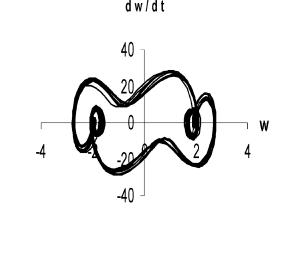
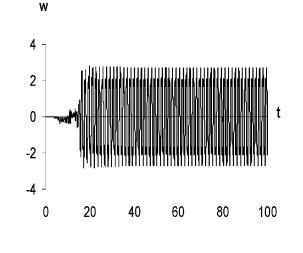
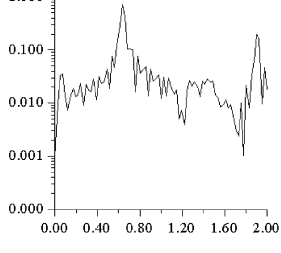
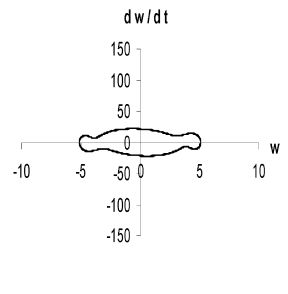
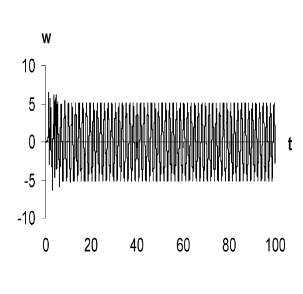
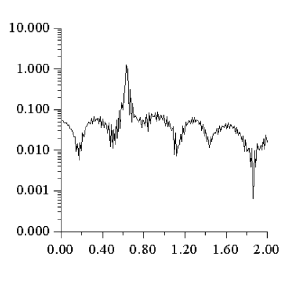
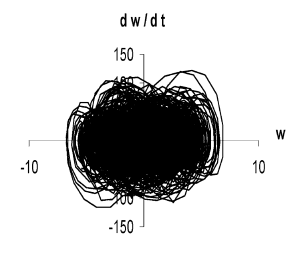
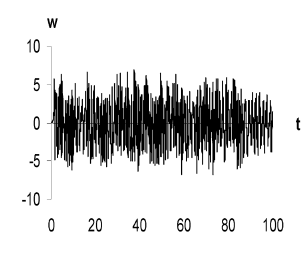
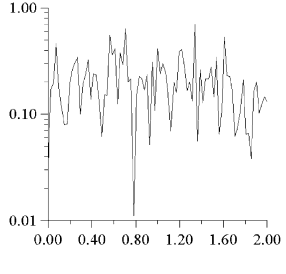


Fig. 2. Maximal deflection $w_{\max}(0.5;0.5)$ vs longitudinal load P_{x_0}

Table 1. Phase portraits, time histories and power spectra for the indicated parameters: **a** $P_{x_0} = 5.65$; **b** $P_{x_0} = 18$

$w = \sum_{i=1}^{M_x=M_y} A_{ij}(t)$ for different numbers of $M_x = M_y$ (see (21), (22))			
(a) $P_{x_0} = 5.65$			
Number of series terms	Phase portrait $w(\dot{w})$	Time history $w(0.5; 0.5; t)$	Power spectrum
1	2	3	4
$M_x=M_y=1$			
$M_x=M_y=3, 5, 7$			
(b) $P_{x_0} = 18$			
$M_x=M_y=1$			
$M_x=M_y=3, 5, 7$			

A similar analysis has been carried out for $P_{x_0} = 18$. Variations in time of the fundamental series terms for the modes $A_{11}(t)$, $A_{13}(t) = A_{31}(t)$, $A_{33}(t)$, $A_{15}(t) = A_{51}(t)$, $A_{35}(t) = A_{53}(t)$ depending on $M_x = M_y$ in (21) and (22) have been also analysed. Beginning with $A_{13}(t)$, all fundamental modes exhibit chaotic vibrations, which can be traced on the phase portraits, the power spectra, Poincaré sections and Lyapunov exponents.

Conclusions

When increasing parameter P_{x_0} , the investigated system starts to lose the regular behaviour, forgetting its initial state, and chaotic dynamics occurs. All used approximations (excluding the first one) exhibit a chaotic vibration state. Series of stiff stability loss are observed. The results obtained for fifth and forty ninth approximations with respect to graph $w_{\max}(P_{x_0})$ are very similar.

In contrary to the Lorenz model, where the most sensitive parameter is represented by the modes number, a similar situation has not been found for our investigated system originated from the von Kármán equations. Namely, a unique system behavior, i.e. a convergence to one solution for all modes (for $P_{x_0} \in [0, 5.5]$) is observed. For $P_{x_0} \in [5.5; 5.75]$, higher approximations converge also to the unique solution. Finally, for $P_{x_0} > 7.5$, higher approximations govern chaotic dynamics. Investigation of the mentioned characteristics yields the following conclusion: each of series term A_{ij} , fully governs vibrations of the system for fixed values of the parameter P_{x_0} . Synchronization of subsystems appears in our analysis. It indicates that beginning with $P_{x_0} > 7.5$ the so called 'multimode' turbulence, i.e. real turbulence, occurs.

References

1. Curry, J.H.; Herring, J.R.; Loncaric, J.; Orszag S.A.: Order disorder in two- and three-dimensional Bernard convection. *J Fluid Mech* 147 (1) (1984) 1–37
2. Franceschnit, V.: Bifurcations of tori and phase locking in a dissipative system of different equations. *Physica D* 6 (3) (1983) 285–304
3. Yahala, H.: Period-doubling cascade in the Rayleigh-Bernard convection. *Progr Theor Phys* 69 (6) (1983) 1802–1810
4. L'vov, V.S.; Predtechenskiy, A.A.; Chernykh, A.I.: Bifurcations and chaos in the system with Taylor's vortices: Real and numerical experiments. *Izvestia VUZov, Radiophysics* 80 (3) (1981) 1099–1121 (in Russian)
5. Dihtiar, V.B.: Stochastic self-vibrations in the system of coupled autogenerators with delay. *Radio-technika Elektronika* 27 (2) (1982) 310–320 (in Russian)
6. Pikovsky, A.S.; Sbitniev, V.I.: Stochasticity in a system of coupled oscillators. Preprint No 641, Leningrad 1981
7. Hogg, T.; Huberman, B.A.: Genetics behavior of coupled oscillators. *Phys Rev A* 29 (1) (1984) 275–281
8. Zhang-Wei; Zhaomiao, L.; Pei, Y.: Global dynamics of a parametrically and externally excited thin plate. *Nonlinear Dyn* 24 (2001) 245–268
9. Lasiecka, I.: Finite dimensionality and compactness of attractors for von Kármán equations with nonlinear dissipation. *Nonlinear Differ Equat Applic* 6 (1999) 437–472
10. Krysko, V.A.; Awrejcewicz, J.; Bruk, V.: On the solution of a coupled thermo-mechanical problem for non-homogeneous Timoshenko-type shells. *J Math Anal Applicat* 273 (2) (2002) 409–416
11. Krysko, V.A.; Awrejcewicz, J.; Bruk, V.: On existence and uniqueness of solution to coupled thermomechanics problem of non-homogenous isotropic plates. *J Appl Anal* 8 (1) (2002) 129–139
12. Awrejcewicz, J.; Krysko, V.A.: *Nonclassic Thermoelastic Problems in Nonlinear Dynamics of Shells*. Berlin Springer-Verlag 2003
13. Awrejcewicz, J.; Krysko, V.A.: Feigenbaum scenario exhibited by thin plate dynamics. *Nonlinear Dyn* 24 (2001) 373–398
14. Awrejcewicz, J.; Krysko, V.A.; Krysko, A.V.: Spatial temporal chaos and solitons exhibited by von Kármán model. *Int J Bifurcation Chaos* 12 (7) (2002) 1465–1513
15. Ruelle, D.: Five turbulent problems. *Physica D* 7 (1/3) (1983) 40–44
16. Goldenweiser A.L.: *Theory of Thin Elastic Shells*. Moscow Gostekhizdat 1953
17. Takens, F.: Dynamical systems and turbulence. In: Rand, D.A., Young, L.-S. (eds) *Lect. Notes in Math.* 898 (1981) 366–381
18. Roux, J.-C.; Simoyi, R.H.; Swinney, H.L.: Observation of a strange attractor. *Physica D* 8 (1/2) (1983) 257–266
19. Krysko, V.A.; Zhelezovskiy, S.E.; Kiritchenko, V.: On convergence speed of the Bubnov-Galerkin method for hyperbolic equations. *Differ Equat* 26 (2) (1990) 323–333 (in Russian)
20. Krysko, V.A.; Zhelezovskiy, S.E.; Kiritchenko, V.: On convergence speed of Bubnov-Galerkin method for one non-classical system of differential equations. *Differ Equat* 23 (8) (1987) 1407–1416 (in Russian)